relatively strong reflector in the 0.2- to 0.5-Hz range, requiring that substantial changes in elastic properties take place over a narrow 5- to 12-km depth interval (*16*, *17*). This constraint means that the major reaction, spinel breakdown, must be pseudounivariant, which is only consistent with perovskite being Al_2O_3-poor at the 660-km discontinuity. In addition, global seismological models (*1*) indicate that the region between 660 and 750 km exhibits steeper velocity-depth gradients than the region below 750 km, which would be consistent with the gradual dissolution of garnet into perovskite accompanied by tie-line rotation. Whichever model is correct, perovskite and magnesiowüstite in peridotite must have similar values of Fe# (0.11) under lower mantle conditions, a fact that impacts physical properties of the mantle such as density and electrical conductivity.

From the standpoint of crystal chemistry, it is interesting and unusual that Al_2O_3 has such a large effect on the Fe content of perovskite. Kesson *et al.* (*18*) observed that perovskites with up to 25 weight % Al_2O_3 could be synthesized at 60 GPa on the join $Mg_3Al_2Si_3O_{12}$-$Fe_3Al_2Si_3O_{12}$ for all values of Fe# between 0.0 and 0.75. Perovskites much richer in Fe and Al than those of this study are therefore stable under deeper mantle conditions. Coupling between Al and Fe may be inferred from comparison with the work of Ito and Takahashi (*19*), who found only 1.3 weight % Al_2O_3 in pure $MgSiO_3$ perovskite, in contrast to 8.9 weight % in $(Mg,Fe)SiO_3$ found by us under the same pressure-temperature conditions. Although the Fe oxidation state in product perovskites is unknown, one possible explanation for the apparent Fe-Al coupling is that a substantial part of the Fe enters as Fe^{3+} through solution of the component $Fe^{III}AlO_3$. This hypothetical perovskite would have Fe^{3+} on the dodecahedral site and Al^{3+} on the octahedral site. The presence of this component seems more likely than the alternative, that small amounts of octahedral Al^{3+} dramatically change the thermodynamic properties of Fe^{2+} on the dodecahedral site.

REFERENCES AND NOTES

1. A. M. Dziewonski and D. L. Anderson, *Phys. Earth Planet. Inter.* **25**, 297 (1981); B. L. N. Kennett, E. R. Engdahl, R. Buland, *Geophys. J. Int.* **122**, 108 (1995).
2. T. Irifune and A. E. Ringwood, *Geophys. Monogr. Am. Geophys. Union* **39**, 231 (1987).
3. A. E. Ringwood, *Geochim. Cosmochim. Acta* **55**, 2083 (1991).
4. E. Ito and E. Takahashi, *J. Geophys. Res.* **94**, 10637 (1989).
5. L. Stixrude, R. J. Hemley, Y. Fei, H. K. Mao, *Science* **257**, 1099 (1992); E. Knittle, R. Jeanloz, G. L. Smith, *Nature* **319**, 214 (1986); J. Ita and L. Stixrude, *J. Geophys. Res.* **97**, 6849 (1992).
6. Starting materials for experiments were mainly ground mixtures of natural minerals from peridotite xenoliths and synthetic magnesiowüstites. Magnesiowüstites $(Mg_{1-x}Fe_x)O$ (x = 0.28 and 0.46) were doped with up to 1 weight % each of Al_2O_3, Cr_2O_3, NiO, and MnO. Magnesiowüstite of x = 0.17 contained about 5 weight % Al_2O_3 and no other dopant. Natural orthopyroxenes contained 3.6 to 4.1 weight % Al_2O_3 and 0.5 weight % CaO in addition to having Fe# values of 0.10 and 0.21. A partially reacted oxide mix of composition $(Mg_{0.9}Fe_{0.1})SiO_3$ without Al_2O_3 was used in one experiment. Natural olivine had the composition $(Mg_{0.896}Fe_{0.104})_2SiO_4$. All starting materials were examined by ^{57}Fe Mössbauer spectroscopy and were found to have an Fe^{3+}/Fe^{2+} ratio of 0.05 or less. Samples were encapsulated in Mo, Re, or Fe capsules and heated at 1600°C {appropriate for 660-km depth [J. M. Brown and T. J. Shankland, *Geophys. J. R. Astron. Soc.* **66**, 579 (1981)]} or 1500°C for 3 hours after pressurization to either 20.4 GPa (for spinel-bearing assemblages) or 25 GPa (for perovskite). Multianvil assemblies and pressure calibrations have been described previously (*13*, *15*). The products were examined by x-ray diffraction, and compositions were determined with the JEOL 8600 electron microprobe at the University of Bristol. All compositions were determined by averaging 10 or more individual point analyses. Experimental data given in Table 1.
7. T. Irifune, *Nature* **370**, 131 (1994).
8. Y. Fei, H-K. Mao, B. O. Mysen, *J. Geophys. Res.* **96**, 2157 (1991).
9. One datum obtained in this study was from a natural $(Mg_{0.896}Fe_{0.104})_2SiO_4$ olivine, which, at 25 GPa and 1600°C, decomposed into a fine intergrowth of perovskite and magnesiowüstite. Because individual crystals were not resolvable with the electron microprobe, the variation of Fe# with Si content was used to extrapolate to end-member compositions in the same manner as that used by Guyot *et al.* (*10*) and Fei *et al.* (*8*). We obtained an Fe# of 0.04 ± 0.02 for perovskite and 0.15 ± 0.02 for magnesiowüstite.
10. F. Guyot, M. Madon, J. Peyronneau, J. P. Poirier, *Earth Planet. Sci. Lett.* **90**, 52 (1988).
11. E. Ito, E. Takahashi, Y. Matsui, *ibid.* **67**, 238 (1984).
12. A. E. Ringwood, *Composition and Petrology of the Earth's Mantle* (McGraw-Hill, New York, 1975).
13. E. A. McFarlane, M. J. Drake, D. C. Rubie, *Geochim. Cosmochim. Acta* **58**, 5161 (1994).
14. B. J. Wood, *J. Geophys. Res.* **95**, 12681 (1990).
15. D. Canil, *Phys. Earth Planet. Inter.* **86**, 25 (1994).
16. H. M. Benz and J. E. Vidale, *Nature* **365**, 147 (1993); A. Yamazaki and K. Hirahara, *Geophys. Res. Lett.* **21**, 1811 (1994).
17. H. Paulssen, *J. Geophys. Res.* **93**, 10489 (1988).
18. S. E. Kesson, J. D. Fitzgerald, J. M. G. Shelley, R. L. Withers, *Earth Planet. Sci. Lett.* **134**, 187 (1995).
19. E. Ito and E. Takahashi, *Geophys. Monogr. Am. Geophys. Union* **39**, 21 (1987).

20. Multianvil experiments were performed at the Bayerisches Geoinstitut under the European Community "Human Capital and Mobility—Access to Large Scale Facilities" programme (contract ERBCHGECT940053 to D.C.R.). B.J.W. acknowledges the support of the Alexander von Humboldt Stiftung during preparation of the manuscript.

13 May 1996; accepted 17 July 1996

Iridium in Natural Waters

A. D. Anbar,* G. J. Wasserburg, D. A. Papanastassiou, P. S. Andersson

Iridium, commonly used as a tracer of extraterrestrial material, was measured in rivers, oceans, and an estuarine environment. The concentration of iridium in the oceans ranges from 3.0 (±1.3) × 10^8 to 5.7 (±0.8) × 10^8 atoms per kilogram. Rivers contain from 17.4 (±0.9) × 10^8 to 92.9 (±2.2) × 10^8 atoms per kilogram and supply more dissolved iridium to the oceans than do extraterrestrial sources. In the Baltic Sea, ~75% of riverine iridium is removed from solution. Iron-manganese oxyhydroxides scavenge iridium under oxidizing conditions, but anoxic environments are not a major sink for iridium. The ocean residence time of iridium is between 2 × 10^3 and 2 × 10^4 years.

Iridium and the other platinum group elements (PGEs) are used as tracers of extraterrestrial material because these elements are enriched in meteorites relative to Earth's crust (*1*). The high concentration of Ir in sediments and rocks at the Cretaceous-Tertiary (K-T) boundary is thought to be the result of an extraterrestrial impact that caused mass extinction (*2*). Smaller Ir enrichments are coincident with other extinction horizons (*3*). The long-term extraterrestrial flux is quantified from the Ir burial flux recorded in deep-sea sediments (*4*). Understanding the aqueous geochemistry of Ir is important because most sediments are deposited in aquatic environments and may be subject to aqueous alteration after deposition. Low concentrations of Ir in natural waters have limited the study of its geochemistry. However, recent advances in negative thermal ionization mass spectrometry (NTIMS) provide the sensitivity to measure Ir in typical crustal materials (*5*). In combination with ultraclean chemical separation techniques, we used isotope dilution and NTIMS to characterize the natural water chemistry of Ir. This method permits the analysis of Ir in as little as 4 liters of water from the open ocean (*6*, *7*), a

A. D. Anbar, G. J. Wasserburg, D. A. Papanastassiou, The Lunatic Asylum of the Charles Arms Laboratory, Division of Geological and Planetary Sciences, California Institute of Technology, Pasadena, CA 91125, USA.
P. S. Andersson, Laboratory for Isotope Geology, Swedish Museum of Natural History, S-104 05 Stockholm, Sweden.

*To whom correspondence should be addressed. Present address: Department of Earth and Environmental Sciences and Department of Chemistry, University of Rochester, Rochester, NY 14627, USA. E-mail: anbar@earth.rochester.edu

Fig. 1. Map of the Baltic Sea showing the sampling stations and the geographic distribution of freshwater inputs. Dashed lines: 40-m depth contour. Dotted lines: 100-m depth contour.

100-fold improvement over earlier methods (*8*). Similar methods are applicable to the other PGEs.

The samples we chose reflect a range of water types, including surface and deep waters in the Pacific Ocean and North Sea, oxic and anoxic waters in the Baltic Sea, and river waters entering the Baltic Sea. The Pacific Ocean was sampled at Station Aloha (22°N, 158°W), where salinity, temperature, dissolved oxygen, and nutrients are routinely analyzed and where conservative and particle-reactive trace elements were recently studied (*9*). The Baltic Sea (Fig. 1) is a 21,000-km^3 estuarine environment in which fresh waters from both pristine and polluted rivers mix with water from the North Sea. The residence time of water in the Baltic Sea is ~40 years. A permanent halocline separates surface waters with salinity of 7 to 8 per mil from bottom waters with salinity of 10 to 13 per mil. The net outflow, governed by surface waters, passes through a narrow, shallow region (the Kattegat), which prevents free exchange between the North Sea and the Baltic Sea. Bottom waters are renewed every 10 years or so when severe storms drive large volumes of seawater through the Kattegat. After renewal, anoxic conditions develop rapidly in deep basins. Baltic hydrology and trace element geochemistry have been studied extensively (*10–14*).

We determined the concentration of Ir (C_{Ir}) at depths of 25 and 1000 m in the open Pacific and at a depth of 80 m in the North Sea (Table 1). The similar Ir concentration in the Pacific Ocean and the North Sea, in the Pacific mixed layer, and at depth in the Pacific suggests that Ir is relatively well mixed in the oceans. The other PGEs vary more with depth (*15*, *16*). The average of our measurements is 4×10^8 atoms kg^{-1} (10^8 atoms kg^{-1} = 1.66×10^{-16} mol kg^{-1}), 10 to 100 times lower than earlier results for near-shore waters off southern California (*8*). Iridium is less abundant in seawater than Pt, Pd, Ru, Rh, Os, or Au (*15*, *17*). Apparently, Ir is the rarest stable element in the oceans.

Table 1. Iridium in natural waters. Analytical precision (±2σ) includes contributions from ion counting statistics propagated through the isotope dilution equation and uncertainties in the chemical blank (*7*). Reproducibility of replicate analyses was within this precision, except when comparing results of procedure 1 with those of procedure 2 in some samples. The slightly higher concentrations determined with procedure 2 cannot be accounted for by contamination. However, procedure 2 can scavenge complexes and particulates not sampled by procedure 1.

Sample and date	Depth (m)	Salinity (per mil)	Ir (10^8 atoms kg^{-1})*
	Seawater		
22°45′ N, 158°00′ W (Pacific Ocean)			
Aloha A†,¶,** (9/94)	25	34.82	3.0 ± 1.3
Aloha A†,¶,** (9/94)	25	34.82	3.4 ± 1.4
Aloha A† (9/94)	25	34.82	5.7 ± 0.8
Aloha C† (9/94)	1000	34.46	4.4 ± 0.6
57°30′ N, 6°59′ E (North Sea)			
H6† (5/91)	80	35.18	3.4 ± 0.6
	Riverwater		
Kalix A‡,** (5/92)	–	–	18.2 ± 1.2
Kalix A‡ (5/92)	–	–	23.5 ± 1.4
Kalix B‡ (6/95)	–	–	17.4 ± 0.9
Neva‡ (5/93)	–	–	49.7 ± 1.3
Vistula‡ (2/93)	–	–	92.9 ± 2.2
	Baltic Sea		
57°20′ N, 20°03′ E			
BY-15 A§,** (5/92)	5	7.30	10.0 ± 1.0
BY-15 A§ (5/92)	5	7.30	11.8 ± 1.2
BY-15 B‡ (5/95)	30	7.23	10.7 ± 1.0
BY-15 C§,** (5/92)	125	9.89	10.9 ± 1.2
BY-15 D§ (5/92)	150	10.45	38.6 ± 2.1
BY-15 E§ (5/92)	225	11.16	38.9 ± 2.2
59°02′ N, 21°05′ E			
BY-28 A‡,** (5/91)	75	7.93	10.9 ± 1.1
BY-28 B‖,#,** (5/90)	50	7.31	14.2 ± 2.0
65°23′ N, 23°30′ E			
F-2‡,** (6/91)	50	3.55	11.3 ± 1.2
	Kattegat-Transition region		
56°40′ N, 12°07′ E			
Anholt‡ (6/95)	15	19.92	25.5 ± 1.5

*10^8 atoms kg^{-1} = 1.66×10^{-16} mol kg^{-1}. †Acidified, unfiltered. ‡Filtered to 0.45 μm, then acidified. §Filtered to 0.10 μm, then acidified. ‖Acidified, then filtered to 0.45 μm. ¶Eight-liter sample volume; all others are ~4 liters. #Average of two analyses. **Iridium separated with procedure 1. Procedure 2 used for all other samples (*6*).

We also determined C_{Ir} in the Kalixälven, Neva, and Vistula rivers, which are representative of freshwaters entering the Baltic Sea. The Kalixälven, which drains Precambrian crystalline rocks in the north, is considered to be pristine (*14*). In this river, C_{Ir} is nearly an order of magnitude higher than in seawater (Table 1). The dissolved metal load is variable during May and June because of variable snowmelt, as indicated by the ~30% difference between the C_{Ir} measurements in May 1992 and June 1995. The concentration of Mn in these samples also varies but is similar to the annual average concentration for this river (*14*). Therefore, we infer that the annual average C_{Ir} is ~20×10^8 atoms kg^{-1}. The Neva and Vistula rivers drain weathered Phanerozoic sedimentary rocks and are polluted by metallurgical industries and coal combustion; therefore, these rivers are enriched in a variety of dissolved components relative to the world river average (*11*). The Ir concentration in these rivers is two to five times that in the Kalixälven and is similar to the concentration in seawater near Los Angeles, California (*8*).

To study the behavior of Ir during estuarine mixing, we made measurements in oxic waters with salinity of 4 to 10 per mil from above the halocline in the Baltic Sea. The concentration of Ir was extremely uniform in these waters (Table 1) and fell well below the conservative mixing line defined by the North Sea and the average Baltic river input (Fig. 2). These observations indicate that ~75% of the dissolved Ir delivered by river water is removed rapidly from solution in the Baltic Sea (*18*), probably into sediments rich in ferromanganese or organic material. Flocculation of Fe-Mn oxyhydroxides is observed

at the river mouths and in the gulfs of the Baltic Sea and influences the transport of other trace metals. Iridium is readily scavenged by ferromanganese phases in seawater and freshwater solutions at pH 7 to 9 (*19*) and is associated with Fe-Mn oxyhydroxides in marine sediments (*16, 20, 21*). In the Baltic Sea, the pH is ≥7.5 and can be >8. Iridium was enriched in a Baltic sample filtered after acidification (BY-28 B), indicating that ~30% of labile Ir is associated with particles larger than 0.45 μm. Manganese-oxyhydroxide is a substantial component of these particles (*11*). The PGEs also have a high affinity for organic compounds and organisms in natural waters (*22*). A large amount of organic material enters the Baltic Sea as humic substances in river waters, and about 75% of this material accumulates in sediments in brackish waters (*13*). The similarity between this figure and the removal of riverine Ir suggests a connection between Ir and organics.

Evidence of Ir scavenging was not seen in the Kattegat, where C_{Ir} fell close to the conservative mixing line (Table 1 and Fig. 2). Although the net flow in this region is outward to the ocean, C_{Ir} in this high-salinity sample is best explained by the mixing of inflowing North Sea water with local river water having a C_{Ir} similar to that of average Baltic river water. Verification of this hypothesis would require measurement of Ir in the rivers draining into the Kattegat. Ir is not significantly depleted in the Kattegat because little Mn and Fe oxide flocculation occurs here; unlike Baltic Sea sediments, Kattegat sediments are predominantly $CaCO_3$ and aluminosilicates (*12*).

To determine whether anoxic sediments are an important sink for Ir, we measured C_{Ir} above and below a well-developed redox boundary in a deep basin (station BY-15). When these samples were collected, the deep waters had been stagnant for 13 years and contained no dissolved oxygen and as much as 110 ml of H_2S per liter. The Ir content in the anoxic waters was four times that in the overlying O_2-saturated waters (Table 1 and Fig. 3). These data show that Ir is not rapidly removed into sediments underlying anoxic waters. This result is consistent with the lack of enrichment of Ir in anoxic marine sediments (*20*).

The cause of the Ir enrichment in anoxic waters is not certain. The observation that C_{Ir} in anoxic waters falls close to the conservative mixing line (Fig. 2) suggests that the initial composition of this water was determined by mixing of seawater and river water in the Kattegat during the preceding renewal event. These events transport water across the bottom of the Baltic in a matter of months. The deep waters are then trapped until the next renewal (*10*). Because the incoming waters travel rapidly and have little or no contact with the oxic, low-salinity regions where ferromanganese sedimentation occurs, they could reach the basin with little loss of Ir. In this case, we can infer that incoming seawater mixes little with Ir-depleted Baltic waters, and that the C_{Ir} of river water entering the Kattegat has not changed in at least the past 13 years.

Alternatively, the enrichment could result from downward transport of Ir bound to Mn-oxyhydroxide particles, followed by dissolution in anoxic waters. This process explains enrichments of Th, Sr, Nd, and Sm at BY-15 (*11*) and is common in anoxic basins (*23*). The similarity of the ratio of ^{232}Th to Ir in oxic and anoxic waters (Fig. 3) indicates that Ir and Th are not strongly fractionated by this process and implies that Ir is as particle-reactive as Th. If true, this is a surprising result. The affinity of a cation for oxyhydroxide surfaces, K_X, scales roughly with the first hydroxide binding constant (β_{1XOH}) (*24*). For Ir^{3+} and Th^{4+}, log β_{1IrOH} = 9.63 and log β_{1ThOH} = 10.80 (*25*). Therefore, $K_{Ir}/K_{Th} \sim (\beta_{1IrOH}/\beta_{1ThOH})$ ~0.1. Additionally, Ir has a tendency to form anionic chloro-complexes, whereas Th does not (*16*). Ir may also be stabilized in solution by the formation of soluble organic complexes. On these grounds, Ir is expected to be substantially less particle-reactive than Th in brackish waters.

The residence time of Ir in the oceans (τ) can be estimated from our data. A lower limit is derived by considering the rate of removal of Ir from seawater. In pelagic sediments, Ir content correlates with Mn, Co, and Ni, elements known to be removed by scavenging (*16, 21*), and Ir is remobilized during the reduction of oxic marine sediments (*20*). Combined with our findings, these observations suggest that the dominant sink of dissolved Ir is scavenging into oxidized deep-sea sediments (hydrogenous scavenging). If the total burial flux of Ir in sediments is F_B, then $\tau = ({}^{SW}C_{Ir}M_o)/(f_BF_BA_o)$, where f_B is the fraction of Ir that is hydrogenous, M_o and A_o are the mass and area of the oceans, respectively, and $^{SW}C_{Ir}$ is the average concentration of Ir in seawater. On the basis of analyses of two deep-sea sediment cores, F_B was $\sim 10^{-16}$ mol cm^{-2} year^{-1} over the past 10^6 years (*21*). Because some of the Ir in deep-sea sediments must be in the form of undissolved aeolian dust and micrometeorites, $f_B < 1$. Therefore, $\tau > 2 \times 10^3$ years.

An upper limit on τ is derived from the inputs of dissolved Ir to the ocean. In this case, $\tau < ({}^{SW}C_{Ir}M_o)/(f_RF_R + f_AF_A + f_MF_M + F_H)$ if we select a reasonable lower bound on each term in the denominator. Here, F_R is the flux of dissolved riverine Ir; f_R is the fraction of this source that reaches the deep ocean; F_A and F_M are the fluxes of Ir on aeolian dust and meteorites, respectively; f_A and f_M are the fractions of these inputs that dissolve; and F_H is the flux of dissolved Ir from deep-sea hydrothermal systems. The Kalixälven has the lowest C_{Ir} of any river studied. We assume that the world's major rivers and the Kalixälven have similar values for C_{Ir}. This similarity holds for Mn. In the Baltic Sea, 25% of riverine Ir survives

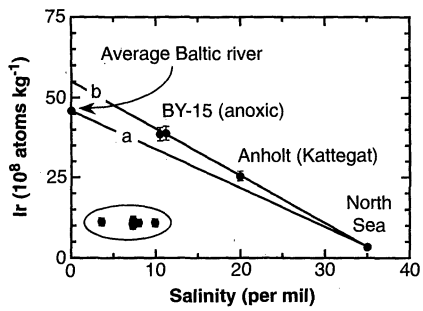

Fig. 2. Iridium in the Baltic Sea. The circled points are samples from BY-15 (oxic), BY-28, and F-2 waters.Curve a is the conservative mixing line between the North Sea and average Baltic river water. The flux-weighted average river concentration is estimated with the assumption that the Kalixälven is representative of the rivers draining Precambrian terrain (226 km^3 year^{-1}) and that the Neva and Vistula are representative of average river water in their drainage basins (112 km^3 year^{-1} and 114 km^3 year^{-1}). The remaining drainage from Phanerozoic terrain (32 km^3 year^{-1}) is assumed to be similar to the Neva. The result, ~46 × 10^8 atoms kg^{-1}, is similar to the concentration in the Neva [49.7 (±1.3) × 10^8 atoms kg^{-1}]. The actual average concentration may be higher because anthropogenic inputs from southern Sweden are neglected. Curve b is the conservative mixing line defined by the samples from the North Sea, Kattegat, and BY-15 anoxic waters.

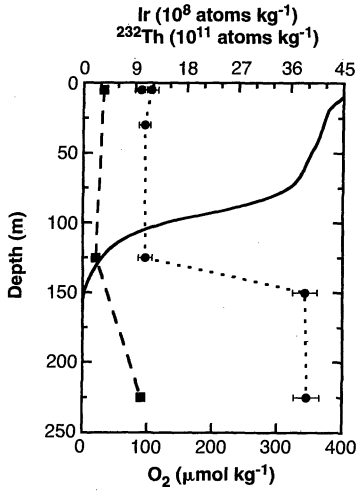

Fig. 3. Iridium (circles and dotted line), ^{232}Th (squares and dashed line), and O_2 (solid line) at station BY-15. The ratio of ^{232}Th to Ir is 210 in oxic waters and 265 in anoxic waters.

scavenging. This value is probably higher in other estuaries because the residence time of water in the Baltic is unusually long; therefore, $f_R > 0.25$ and $f_R F_R > 35$ mol year^{-1} (*26*). On the basis of mineral aerosol flux estimates (*27*), F_A is ~240 mol year^{-1} if we assume that these aerosols have a composition similar to average continental crust. F_M equals 70 ± 35 mol year^{-1}, on the basis of direct measurements of the meteorite flux (*28*), if we assume a chondritic average meteorite composition. Both f_A and f_M are unknown but may be small because of the low solubility of Ir carrier phases such as metals and sulfides. Gold and the PGEs have similar distributions in crustal rocks and similar chemical reactivity. About 3% of aerosol-borne Au is believed to dissolve (*17*). It is reasonable to assume a similar value for f_A. From the Os isotope composition of marine ferromanganese leachates, it is known that $0 \leq f_M \leq 0.2$ (*29*). The magnitude of F_H is unknown, but could be low if Ir is scavenged by Fe-oxyhydroxides formed during the cooling of hydrothermal plumes. For these limits, $(f_R F_R + f_A F_A + f_M F_M + F_H) > 42$ mol year^{-1}, with $f_R F_R$ the dominant term. Thus, 2×10^3 years $< \tau < 2 \times 10^4$ years. This range is similar to the values for many trace metals that are moderately particle-reactive (*30*).

These estimates show the importance of terrestrial sources to the ocean Ir budget. Even if $f_M = 0.2$, Ir dissolved in rivers accounts for >60% of the soluble Ir delivered annually to the oceans and >10% of the total flux of Ir to deep-sea sediments (including particulates). Hydrogenous, terrestrial Ir may approach 50% of this flux in regions of low aeolian input. However, massive meteorite impacts may be large, episodic sources of Ir to seawater if a substantial fraction of impactor Ir is vaporized and enters the ocean in dissolved form.

The sensitivity of Ir removal from natural waters to redox conditions, pH, and salinity indicates that Ir can be remobilized and concentrated into certain types of sediments. This could lead to modest Ir enrichments in the sedimentary record without requiring exogenous Ir. However, at the K-T boundary, the globally integrated quantity of Ir in sediments is ~10^3 times the total amount of Ir in seawater (*2*, *31*). This comparison highlights the singular nature of the K-T enrichment. The only terrestrial source reasonably capable of supplying this quantity of Ir is an extended period of volcanism. The time span of 10^4 to 10^5 years represented by the Ir anomaly in the K-T section at Gubbio, Italy, has been cited as evidence for such a source rather than a sudden, exogenous input (*32*). It has also been suggested that this span is the result of bioturbation, diffusion, or weathering of Ir-enriched fallout on the continents. However, on the basis of our estimate of the Ir residence time in the oceans, an impact-derived Ir anomaly could persist for such a time span if dissolved extraterrestrial Ir from this event overwhelms terrestrial sources and is incorporated into sediments by hydrogenous scavenging. Therefore, the width of the Ir anomaly in some K-T sections can be explained without invoking secondary alteration or extended periods of Ir input to the oceans.

REFERENCES AND NOTES

1. Chondritic Ir abundance: 481 parts per billion [compilation by E. Anders and N. Grevesse, *Geochim. Cosmochim. Acta* **53**, 197 (1989)]. Crustal Ir abundance: 50 parts per trillion [B. K. Esser and K. K. Turekian, *ibid.* **57**, 3093 (1993)].
2. L. W. Alvarez, W. Alvarez, F. Asaro, H. V. Michel, *Science* **208**, 1095 (1980).
3. F. T. Kyte, Z. Zhou, J. T. Wasson, *Nature* **292**, 417 (1981); W. Alvarez, F. Asaro, H. V. Michel, L. W. Alvarez, *Science* **216**, 886 (1982); P. E. Playford, D. J. McLaren, C. J. Orth, J. S. Gilmore, W. D. Goodfellow, *ibid.* **226**, 437 (1984); X. Dao-Yi *et al.*, *Nature* **314**, 154 (1985); C. J. Orth, M. Attrep, X. Y. Mao, *Geophys. Res. Lett.* **15**, 346 (1988); K. Wang *et al.*, *Geology* **19**, 776 (1991).
4. J. L. Barker and E. Anders, *Geochim. Cosmochim. Acta* **32**, 627 (1968); F. T. Kyte and J. T. Wasson, *Science* **232**, 1225 (1986).
5. K. G. Heumann, in *Inorganic Mass Spectrometry*, F. Adams, R. Gijbels, R. van Grieken, Eds. (Wiley, New York, 1988), pp. 301–376; R. A. Creaser, D. A. Papanastassiou, G. J. Wasserburg, *Geochim. Cosmochim. Acta* **55**, 397 (1991); J. Völkening, T. Walczyk, K. G. Heumann, *Int. J. Mass Spectrom. Ion Processes* **105**, 147 (1991).
6. Four-liter samples were acidified (0.024 M HCl) and spiked with separated ^{191}Ir for isotope dilution. They were then oxidized by means of bubbling with Cl_2 gas. On thermodynamic grounds, Ir from both the sample and spike is expected to be in the form $IrCl_6^{2-}$ under these conditions (*8*, *20*), facilitating equilibration with the spike. Ir was separated with one of two procedures. In procedure 1, samples were loaded directly onto 1-ml anion-exchange resin columns and eluted in 6 M HCl after reduction on the column with an SO_2 solution. In procedure 2, coprecipitation of Ir with iron oxyhydroxide was used as an initial separation step, followed by anion-exchange separation and SO_2 elution. Yields through this stage were 80 to 90%. Residual organics were decomposed with $HClO_4$-HNO_3, ultraviolet irradiation, or both. Residual salts were removed by a 5-μl anion column. Overall yields were 50 to 75%. The separated Ir was loaded with $Ba(OH)_2$ on a Ni filament and analyzed as IrO_2^- (masses 223 and 225) in a Lunatic mass spectrometer equipped with an electron multiplier for ion counting. Ionization efficiencies were 0.1 to 0.3%. No background was observed nor were there any interferences at the measured masses. Detailed procedures are presented elsewhere [A. D. Anbar, thesis, California Institute of Technology (1996); A. D. Anbar *et al.*, manuscript in preparation].
7. For the separation of Ir from a 4-liter sample, the blank corrections were $(5 \pm 5) \times 10^8$ atoms for procedure 1, and $(2 \pm 2) \times 10^8$ atoms for procedure 2. The blank values are consistent with the Ir content of reagents and with the content measured in waters from which Ir was previously separated. An additional blank of ~5×10^7 atoms was introduced by the use of $HClO_4$ to decompose organics. This treatment was needed only for river water samples and for anoxic waters. Procedure 2 is preferred and is necessary for large-volume samples bearing little Ir as well as for samples with large amounts of dissolved organics or metals; these tend to precipitate or coagulate upon chlorination, rendering procedure 1 impractical. No significant blank was detected in clean waters handled alongside samples during all shipboard manipulations and storage. Filament loading blanks were $<10^6$ atoms.
8. J. Fresco, *Talanta* **32**, 830 (1985); V. Hodge, M. Stallard, M. Koide, E. D. Goldberg, *Anal. Chem.* **58**, 606 (1986).
9. Waters from the Pacific Ocean were collected in collaboration with the Hawaiian Ocean Time series project in September 1994 [HOT-57; research vessel (R.V.) *Moana Wave*]. Waters from the Baltic Proper, the Kattegat, the Gulf of Bothnia, and the North Sea were collected aboard the R.V. *Argos* (Fishery Board of Sweden) from 1991 to 1995 in collaboration with the Swedish Meteorological and Hydrological Institute. All samples were collected in polyvinyl chloride Niskin bottles with Teflon-coated inner springs or with Teflon-coated GO-FLO bottles and stored in acid-cleaned polyethylene bottles acidified to ~0.025 M HCl. Pacific Ocean and North Sea waters were stored without filtration. Baltic Sea and river waters were filtered in the field (≤0.45 μm) before acidification. D. M. Karl and C. D. Winn, *Environ. Sci. Tech.* **25**, 1977 (1991); A. D. Anbar, R. A. Creaser, D. A. Papanastassiou, G. J. Wasserburg, *Geochim. Cosmochim. Acta* **56**, 4099 (1992); M. Roy-Barman, J. H. Chen, G. J. Wasserburg, *Earth Planet. Sci. Lett.* **139**, 351 (1996).
10. Reviews of Baltic Sea hydrology: M. Falkenmark and Z. Mikulski, *Nord. Hydrol.* **6**, 115 (1975); S. Bergström and B. Carlsson, *Ambio* **23**, 280 (1994).
11. On trace elements in the Baltic Sea: P. S. Andersson, G. J. Wasserburg, J. Ingri, *Earth Planet. Sci. Lett.* **113**, 459 (1992); ———, M. C. Stordal, *ibid.* **124**, 195 (1994); P. S. Andersson, G. J. Wasserburg, J. H. Chen, D. A. Papanastassiou, J. Ingri, *ibid.* **130**, 217 (1995).
12. On the geochemistry of Baltic Sea sediments: J. Ingri, thesis, Lulea University of Technology, Sweden (1985); R. O. Hallberg, *Ambio* **20**, 309 (1991); F. Belmans, R. van Grieken, L. Brügmann, *Mar. Chem.* **42**, 223 (1993).
13. On organics in the Baltic Sea: F. Wulff and A. Stigebrandt, *Global Biogeochem. Cycles* **3**, 63 (1989).
14. C. Pontér, J. Ingri, K. Boström, *Geochim. Cosmochim. Acta* **56**, 1485 (1992).
15. D. S. Lee, *Nature* **305**, 47 (1983); E. D. Goldberg, M. Koide, J. S. Yang, K. K. Bertine, in *Metal Speciation: Theory, Analysis, and Application*, J. R. Kramer and H. E. Allen, Eds. (Lewis, Chelsea, MI, 1988), pp. 201–217; J. S. Jacinto and C. M. G. van den Berg, *Nature* **338**, 332 (1989); K. K. Bertine, M. Koide, E. D. Goldberg, *Mar. Chem.* **42**, 199 (1993); M. Koide, E. D. Goldberg, R. Walker, *Deep-Sea Res. II* **43**, 53 (1996).
16. E. D. Goldberg, V. Hodge, P. Kay, M. Stallard, M. Koide, *Appl. Geochem.* **1**, 227 (1986).
17. K. K. Falkner and J. M. Edmond, *Earth Planet. Sci. Lett.* **98**, 208 (1990).
18. The Baltic Sea is divided into two boxes separated by the permanent halocline. River water and seawater enter box 1 and box 2, respectively, and water exits box 1 to the ocean. Because salinity (S_i) is conserved, $M_{rw}S_{rw} + M_{21}S_2 = M_{out}S_1 + M_{12}S_1$ and $M_{sw}S_{sw} + M_{12}S_1 = M_{21}S_2$, where M_i are water mass fluxes, and the subscripts sw, rw, 12, 21, and out denote inputs of seawater and river water, exchange between boxes, and the flux out from box 1, respectively. $S_{rw} \sim 0$ per mil, $S_{sw} = 35$ per mil, $S_1 = 8$ per mil, $S_2 = 12$ per mil, and $M_{rw} = 446$ km^3 year^{-1}. By imposing mass conservation (that is, $M_{sw} + M_{12} = M_{21}$; $M_{rw} + M_{21} = M_{out} + M_{12}$), the remaining mass fluxes can be calculated. These fluxes are combined with observations of Ir in seawater, river water, and box 1 ($C_{sw} = 3.4 \times 10^8$ atoms kg^{-1}; C_{rw} is ~50×10^8 atoms kg^{-1}; $C_1 = 10.5 \times 10^8$ atoms kg^{-1}) to determine the flux into sediments (F_{sed}) by using the equations $M_{rw}C_{rw} + M_{21}C_2 = M_{out}C_1 + M_{12}C_1 + F_{sed}$ and $M_{sw}C_{sw} + M_{12}C_1 = M_{21}C_2$. $F_{sed} = 1.7 \times 10^{24}$ atoms year^{-1}, compared with a riverine Ir flux of 2.2×10^{24} atoms year^{-1}.
19. To study scavenging of Ir by Mn and Fe oxyhydroxides, solutions containing ≈5×10^{-6} mol of Ir per kilogram and 10 to 100 parts per million of Fe or Mn were prepared with Fe, Mn, and Ir chloride salts dissolved in ~250 ml of either pure water or seawa-

ter at pH 2 to 4. These were titrated to pH ≥6 to generate precipitates. The solutions were agitated repeatedly over 2 to 240 hours, and the pH was adjusted to compensate for acidification from cation hydrolysis. Filtered aliquots of the solutions were spiked with a ^{191}Ir-enriched tracer and analyzed by isotope dilution inductively coupled plasma mass spectrometry (ICP-MS). Both Fe and Mn particles scavenged >50% of the Ir at alkaline pH, in both freshwater and seawater. Scavenging efficiency increased with increased pH, consistent with cation adsorption. Increased scavenging in freshwater probably reflects a shift in speciation from anionic chloro-complexes to hydroxy- and mixed hydroxy-chloro–complexes that are more readily scavenged.
20. D. C. Colodner, E. A. Boyle, J. M. Edmond, J. Thomson, *Nature* **358**, 402 (1992).
21. L. Zhou and F. T. Kyte, *Paleoceanography* **7**, 441 (1992); F. T. Kyte, K. Leinen, R. G. Heath, L. Zhou, *Geochim. Cosmochim. Acta* **57**, 1719 (1993).
22. M. C. Wells, P. N. Boothe, B. J. Presley, *Geochim. Cosmochim. Acta* **52**, 1737 (1988); J. Li and R. H. Byrne, *Environ. Sci. Tech.* **24**, 1038 (1990); S. A. Wood, *Can. Mineral.* **28**, 665 (1990); ———, C. D. Tait, D. Vlassopoulos, *Geochim. Cosmochim. Acta* **58**, 625 (1994).
23. D. W. Spencer and P. G. Brewer, *J. Geophys. Res.* **76**, 5877 (1971); S. Emerson, R. E. Cranston, P. S. Liss, *Deep-Sea Res.* **26A**, 859 (1979).
24. D. Dzombak and F. M. M. Morel, *Surface Complexation Modelling* (Wiley, New York, 1990); Y. Erel and J. J. Morgan, *Geochim. Cosmochim. Acta* **55**, 1807 (1991).
25. H. Gamsjäger and P. Beutler, *J. Chem. Soc. Dalton Trans.*, **1979**, 1415 (1979); C. F. Baes and R. E. Mesmer, *The Hydrolysis of Cations* (Krieger, Malabar, FL, 1986).
26. A global river water flux of 4.2 × 10^4 km^3 year^{-1} is used [M. I. Lvovitch, *Eos* **54**, 28 (1973)].
27. R. A. Duce *et al.*, *Global Biogeochem. Cycles* **5**, 193 (1991).
28. S. G. Love and D. E. Brownlee, *Science* **262**, 550 (1993).
29. B. K. Esser and K. K. Turekian, *Geochim. Cosmochim. Acta* **52**, 1383 (1988).
30. K. W. Bruland, in *Chemical Oceanography*, J. P. Riley and R. Chester, Eds. (Academic Press, London, 1983), vol. 8, pp. 157.
31. C. B. Officer, A. Hallam, C. L. Drake, J. D. Devine, *Nature* **326**, 143 (1987).
32. R. Rocchia *et al.*, *Earth Planet. Sci. Lett.* **99**, 206 (1990).
33. R. A. Creaser contributed to the development of the analytical methods. We thank D. Karl and others involved in the HOT program for help in sampling the Pacific Ocean, M. Roy-Barman and D. Porcelli for their assistance in the field, and G. Ravizza for his thoughtful comments. Supported by U.S. Department of Energy grant DE-FG03-88ER13851, NASA grant NAGW-3337, and by an NSF Graduate Research Fellowship to A.D.A. Ship time on the R.V. *Moana Wave* was supported by NSF OCE-9303094 (R. Lukas) and OCE-9301368 (D. Karl). Division contribution number 5669 (931).

26 April 1996; accepted 17 July 1996

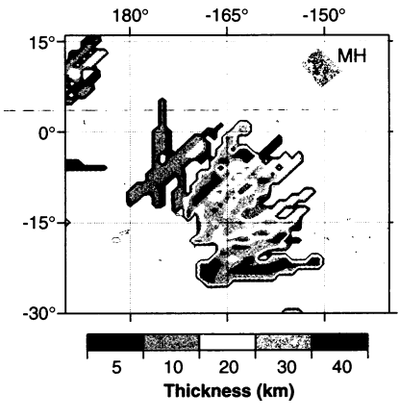

Fig. 1. Map view of the inferred thickness of the low-velocity anomaly, as constrained by $SP_{diff}KS$ ray results. Because the energy of diffracted *P* waves along the CMB is constrained to lie predominantly in the lowermost 50 km of the mantle, the thickness of this feature may be estimated from a combination of the observed time of arrival and length of travel of this phase along the CMB and waveform analyses [(*1*)]. MH denotes the location of the anomaly characterized by Mori and Helmberger using precursors to the reflected *PcP* phase (*2*).

Seismic Evidence for Partial Melt at the Base of Earth's Mantle

Quentin Williams* and Edward J. Garnero

The presence of an intermittent layer at the base of Earth's mantle with a maximum thickness near 40 kilometers and a compressional wave velocity depressed by ~10 percent compared with that of the overlying mantle is most simply explained as the result of partial melt at this depth. Both the sharp upper boundary of this layer (<10 kilometers wide) and the apparent correlation with deep mantle upwelling are consistent with the presence of liquid in the lowermost mantle, implying that the bottom of the thermal boundary layer at the base of the mantle may lie above its eutectic temperature. Such a partially molten zone would be expected to have enhanced thermal and chemical transport properties and may provide constraints on the geotherm and lateral variations in lowermost mantle temperature or mineralogy.

Recent seismic observations show that the base of Earth's mantle has anomalously slow *P*-wave velocities (*1*, *2*). Evidence for a discrete layer is provided by two independent data types: (i) *SKS* waves that couple with short segments of core-diffracted *P* waves (*1*) and (ii) precursors to the core-reflected *PcP* phase (*2*). This layer is within the thermal boundary between the mantle and the core; depending on its origin, it may strongly influence the geomagnetic field, and it likely affected the evolution and differentiation of the deep Earth. The *P*-wave velocity in this layer is reduced by at least 10% relative to that in the mantle, with its thickness varying between ~5 and 40 km (*1*). Seismological data also imply that the transition between the basal layer and the overlying mantle is (at least locally) sharp [less than 10 km wide (*2*)]. The layer is thick beneath a region where the lower mantle has large-scale slower-than-average velocities (such as the central Pacific: Fig. 1) and is undetectable below average or faster-than-average lower mantle material (such as the circum-Pacific) (*1*), implying a relation with hot upwellings in the deep Earth.

Three phenomena could produce this anomalous basal layer: (i) partial melting, (ii) a chemical discontinuity, or (iii) a phase transition in mantle material near a pressure of 135 GPa, corresponding to depths just above the core-mantle boundary (CMB) (*3*). Although the first two possibilities are not exclusive, the last possibility is unlikely. Both Mg-rich silicate perovskite and $CaSiO_3$-perovskite appear to be stable at pressures spanning those present within most of the mantle (*4*, *5*); no significant phase transition is observed in (Mg,Fe)O in this pressure range (*6*), and the $CaCl_2$ structure of SiO_2 is apparently stable to pressures in excess of 130 GPa (*7*).

Thus, it appears that only a change in chemistry or the presence of melt can account for this reduction in seismic velocity. We first examined the possible origins of a change in melt fraction 40 km above the CMB. The amount of melt that can produce a 10% decrease in *P*-wave velocity may be estimated from the limited data set on elastic properties of silicate melts and their pressure dependence (*8*, *9*), coupled with treatments of the elastic behavior of two-phase aggregates (*10*, *11*). An upper bound on the effect of an Fe-rich fluid intercalated in the lowermost mantle may be derived if one assumes that the fluid has the properties of the outer core. If the fluid is instead an ultramafic silicate melt, its bulk modulus (*K*) under CMB conditions is uncertain but is likely to lie close to that of the solid mantle at these depths (*8*). Coincidentally, the *K* of core fluid is also close to that of the solid mantle at the CMB [644 GPa versus 653 GPa (*12*)]. We assumed that the *K* of the melt is equivalent to that of coexisting solid silicate mantle material. To estimate the size of the velocity change associated with the presence of partial melt, we also inferred the aggregate density. The density change associated with the melting of silicates at high pressures is

Earth Sciences Board and Institute of Tectonics, University of California, Santa Cruz, CA 95064, USA.

*To whom correspondence should be addressed.